Louis Savein Dupuis Journal of Multidisciplinary Resaerch 2023, 2: 32-37
Doi.: 10.21839/lsdjmr.2023.v2.24

Research Article

Sensor properties of heterocyclic compound with nanoparticles – molecular docking studies

J. Lesy Josephine, K.Thanikamani, P. Ramanathan

Department of Chemistry ,Immaculate college for women, Chinnakanganankuppam

Department of Chemistry, Government College of Arts and Science, Thiruchirappalli

Department of Chemistry, Thanthai Hans Roever College, Perambalur

*****Corresponding author (E.mail: lesyjosephine.s@gmail.com)

Abstract

Quenching and enhancing behaviourof 1-(4-methoxyphenyl)-2-(4-methylnaphthalen-1-yl)-1H-phenanthro[9,10-d]imidazole (MMPI) with Cu –doped ZnO nanoparticle has been studied. MMPI has been characterized by ^{1}H, ^{13}C NMR and mass spectral analysis. Cu –doped ZnO nanoparticle have been synthesised by sol-gel method and characterized by powder X-ray diffraction (XRD), Scanning Electron Microscope (SEM) and Energy Dispersive X-ray Spectra (EDS).Quenching and enhancing behaviour were confirmed by the MMPI strongly binding on the surface of Cu –doped ZnO nanoparticle. Increasing concentration of nanoparticle into MMPI results in enhances absorbance and quenching fluorescence was observed. Fluorescence quenching was confirmed electron transfer from excited state of MMPI to nanoparticle. Theoretical calculations were performed by Gaussian -03 package. In order to understand the binding interaction with DNA docking study has been carried out.

Keywords: :*MMPI; Cu –doped ZnO; XRD, SEM, EDS; Docking studies*

Introduction

Tunable multicolour emissions natured materials have arriving significant notice for their opto-electronics as prospective light emitting displays [Baker, *et al.*, (2010), Jaiswal, *et al.*, (2012)] and biological characterisation [Reineke. S, *el at., (2009)*]. There are three kinds of materials are used to construct multicolour emission [Vanithakumari.S, *et al., (2009)* – Wang. X *et al., (2011)*], they areorganic dye-doped semiconducting polymer nanoparticles, quantum dots of different sizes and lanthanide-doped, nanomaterials.A wide band gap of 3.37 eV (at 300 K) is gained by ZnO,itis vital II-VI semiconductor and due to electron hole recombination it emits illumination in the range of 375–405 nm.Because of defect or trapped states it gives green emission at 545 nm.Due to alone ionized oxygen position in the ZnO nanocrystals the green emissionisoriginated. Because of its nontoxicity and chemical stability the great consideration for bio-imaging applications is achieved by ZnO nanocrystals.Effectively tuned from blue to yellow [8, 9] is by the emission of nanostructuredZnO.Yellowemission is very bright compared to blue emission.Blue emission of the ZnOnanosemiconductor has not been better projection in biological labelling as compared to thegreen and yellow emissions.Applications for these new classes of materialshave been inspired for some intensive investigations. Variety of materials like cerium, zinc, and iron oxides, titanium can be composed of metal oxide nanoparticles [Johnston. H.J, *et al., (2009)*]. The yielding is entirely new and different physico-chemical properties as there are changes in their fundamental physical and chemical and properties causes a major change in the size of such particle. These particles widely used for gas sensors, non-linear optics, catalysis, cosmetics varistors, pigments, solar energy exchange, etc. [Sakohapa. S *et al.,(1992)* –Hara. K *et al., (2000)*]. ZnO has been calculated in transparent UV protection films, transparent conductors, chemical sensors and varistorsand so on as a large band gap semiconductor [Cao *etal., (2000)*, Bagnall.M *et al.,(1998)*]. The report as Xia et al is forPolymer-stabilized nanoZnO with blue emission[Xiong. H et al., (2006)] and the cell imaging is obtained by tunable photoluminescence with and the ZnO@polymer core–shell nanoparticles [Xiong.H *et al.*, ,Subramanian. V *et al.,(2003)*].Using single crystals or polycrystalline of Co^{2+} :ZnO prepared by pellet sintering many scholars identified the visible photo-response of Co-doped ZnO. They found that the nickel-doped ZnO hollow spheres exhibited only weak ferromagnetism at 300 Kwhereas Co-doped ZnO hollow exhibited ferromagnetism at room temperature. Not due to any cobalt oxide phase formation or any metallic Co segregation the observed nature of ferromagnetism was intrinsic.By Tao Liu et al.,Herein about 5 nm in size the Co-doped ZnO nanoparticles were synthesized and we report the binding interaction and surface behaviour of ZnO nanoparticles by MMPI, unfortunately results by the spectral studies were unexpected. Fluorescence quenching results which is obtained is an unique study of interaction between Cu -doped ZnO and 1-(4-methoxyphenyl)-2-(4-methylnaphthalen-1-yl)-1H-phenanthro[9,10-d] imidazole.

Experimental

Synthesis of 1-(4-methoxyphenyl)-2-(4-methylnaphthalen-1-yl)-1H-phenanthro[9,10-d] imidazole

4-methyl-1-naphthaldehyde (1 mmol), phenanthrene-9,10-dione (1 mmol), 4-methoxyaniline (1 mmol) and NH_4OAc (1mmol) with borontriflurideethyletharate (1 mol%) as catalyst was stirred at 80 °C for 2 hrs. The movement of the reaction was monitored by TLC (Scheme 1). After end of the reaction the mixture was cooled, dissolved in dichloromethane and filtered. The product was purified by column chromatography using benzene: hexane (9:1) as the eluent. The newly synthesised 1-(4-methoxyphenyl)-2-(4-methylnaphthalen-1-yl)-1H-phenanthro[9,10-d] imidazole have been characterised by $^{1}H$and ^{13}C NMR and mass spectral analysis. M.p. 278 ºC., Anal. calcd. for $C_{33}H_{24}N_2O$: C, 85.32; H, 5.21; N, 6.03. Found: C, 85.29; H, 5.20; N, 6.01. ^{1}H NMR (400 MHz,

DMSO): δ 2.32 (s, 3H), 3.72 (s, 3H), 8.94 (d, J = 8.4 Hz, 1H), 8.91 (d, J = 8.4 Hz, 1H), 8.68 (d, J = 7.6 Hz, 1H), 7.88 (d, J = 8.0 Hz, 1H), 7.76 (d, J = 7.2 Hz, 1H), 7.56 (d, J = 7.6 Hz, 1H), 7.39 (t, 1H), 7.21 (d, J = 8.0 Hz, 1H), 6.95 (d, J = 8.4 Hz, 2H), 7.97 (t, 2H), 7.68 (t, 2H), 7.55-7.42 (m, 5H). ^{13}C NMR (400 MHz, DMSO): δ 21.31, 55.28, 114.62, 120.27, 121.98, 122.59, 123.66, 124.42, 124.67, 125.19, 125.60, 125.78, 126.20, 126.69, 126.82, 126.86, 127.24, 127.42, 127.64, 128.04, 128.09, 128.29, 128.41, 129.50, 129.52, 129.72, 129.95, 132.35, 132.76, 136.28, 150.47, 159.47. m/z. 464.56 [M+].

Synthesis of Cu-doped ZnO by Sol-gel method

To the zinc acetate (0.1g) solution with copper nitrate in 10ml 0.01 M polyvinyl pyrrolidone K-30, freshly prepared solution of 1:1 aq. ammonia was added slowly to reach a pH of 7, under constant stirring. The stirring was continued for another 30 minutes to get a gel. The formed glassy like white gel was permitted to overnight. It was filtered and washed with water a number of times, dried at 100 °C for 1 hrs and calcinated at 400 °C for 3 hrs to pale grey solid.

Measurements

The ^{1}H and ^{13}C NMR spectra at 400 and 100 MHz, respectively were obtained at room temperature using a Bruker 400 MHz NMR spectrometer (Bruker biospin, California, USA). The mass spectra were obtained using a Thermo Fischer LC-Mass spectrometer in fast atom bombardment (FAB) mode (Thermo, France). XRD patterns were recorded for the centrifuged and dried samples using X–ray Rigakudiffractometer with Cu K_α source (30 kV, 100 mA), at a scan speed of 3.0000 deg/min, step width of 0.1000 deg, in a 2θ range of 20-80°. The energy dispersive X-ray (EDS) spectra of the nanosemiconductors were recorded with a JEOL JSM-5610 scanning electron microscope (SEM) equipped with back electron (BE) detector and EDX. The sample was placed on an adhesive carbon slice supported on copper stubs and coated with 10 nm thick gold using JEOL JFC- 1600 auto fine coater prior to measurement. The binding relations of MMPI with nanoparticles has been recorded using UV–vis spectroscopy by employing a Systronics Double beam UV–vis spectrophotometer operated on 200–800 nm wavelengths. The fluorescence measurements have been carried out with a Perkin Elmer LS45 spectrofluorimeter. DFT calculations were performed with Gaussian-03 [Frisch. M *et al., (2004)*] package.

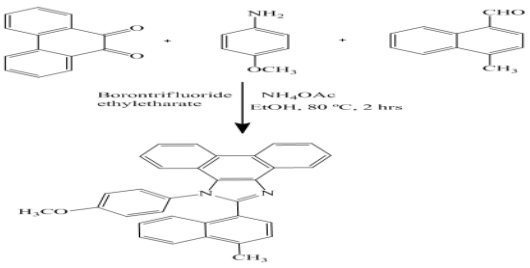

Synthetic route of 1-(4-methoxyphenyl)-2-(4-methylnaphthalen-1-yl)-1H-phenanthro[9,10-d]imidazole

Molecular docking studies

The structure of ct-DNA is composed two strands that wrap around each other to form a right-handed double helix with the B-form. The crystal structure of B-DNA [$(CGCGAATTCGCG)_2$] is used in molecular docking were extracted from Protein Data Bank (http://www.rcsb.org/pdb). MGL tools 1.5.4 with AutoGrid4 and AutoDock4 were used to perform the docking calculations between 1-(4-methoxyphenyl)-2-(4-methylnaphthalen-1-yl)-1H-phenanthro[9,10-d]imidazole and DNA sequence. The structure of 1-(4-methoxyphenyl)-2-(4-methylnaphthalen-1-yl)-1H-phenanthro[9,10-d]imidazole was saved in MOL file and used for docking. Receptor (DNA) and 1-(4-methoxyphenyl)-2-(4-methylnaphthalen-1-yl)-1H-phenanthro[9,10-d]imidazole (drug) files were provided using AutoDock Tools. All of the hetero atoms, water molecules and other unwanted ions were removed from B-DNA using Discovery Studio 4.0 [21]. The polar hydrogen atoms, partial atomic charges and Gasteiger charges of DNA were added to the compound by AutoDock Tools [Morris. G *et al., (1998)*, Morris. G *et al., (2009)*] before subjecting to docking analysis. Ligand docking calculations were carried out using Lamarckian genetic algorithm (LGA) [Huey, *et al., (2007)*]. The DNA molecule was enclosed in a box with number of grid points of 126 x 126 x 126 was created along the x, y and z axis and a grid spacing of 0.375 Å, i.e., blind docking was performed. The output structures of the docked molecules were further analyzed with PyMOL software package [De Lano, *et al., (2004)*].

Results and discussion

XRD and SEM analysis Cu -doped ZnO nanoparticle

X-ray diffraction pattern (XRD) of (Figure 1) Cu -doped ZnO nanoparticle obtained by sol-gel method. The diffraction patterns match with the standard JCPDS card number (89-7102). The crystal structure of Cu -doped ZnO are primitive hexagonal with crystal constants a and b as 3.253 Å and c as 5.029 Å. In the case of doping with copper, as the radii of Zn^{2+} and Cu^{2+} are similar, Cu^{2+} can change Zn^{2+} in the pattern without vary in the pattern parameters. The XRD of Cu -doped ZnOfails to present any peak other than those of ZnO. The average crystallite sizes (L) of the sol–gel synthesized Cu- doped ZnO have been deduce as 25 nm, respectively. They have been obtained from the full width at half maximum (FWHM) of the most intense peaks of the individual crystals by the Scherrer equation, L = 0.9 λ/βcosθ, where λ is the wavelength of the X-rays used, θ is the diffraction angle and β is the full width at half maximum of the peak. Calculated surface area for Cu- doped ZnOis 39.54 m^2/g.The scanning electron micrographs (SEM) of Cu -doped ZnO nanoparticleare shown in figure 2. The EDS spectra are shown in figure 3, presence of zinc, oxygen, copper signals confirms the purity of the synthesized Cu–doped ZnO nanoparticle.

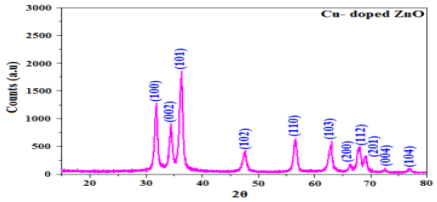

X-ray diffraction pattern of (XRD) of Cu- doped ZnO nanoparticle

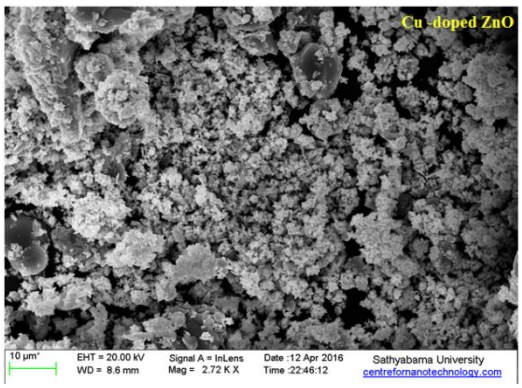

SEM images of Cu- doped ZnOnanoparticle

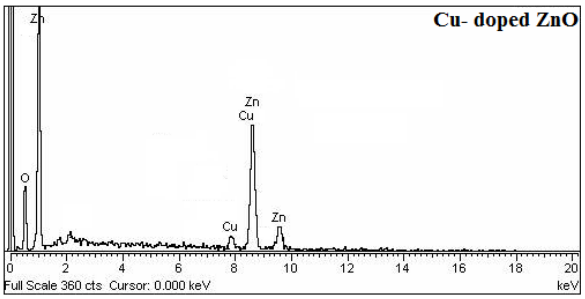

EDX spectra of Cu- doped ZnOnanoparticle

Absorption and emission behaviour of MMPI with Cu -doped ZnO

The absorption spectra of MMPI in the presence and absence of nanoparticle are shown in figure 4. The nanoparticle enhances the absorbance of MMPI which indicate the nanocrystals do not adjust the excitation of the ligand. The enhanced absorption at 257 nm is due to adsorption of the MMPI on nanoparticle surface and effective electron transfer from the excited MMPI to the conduction band (CB) of the nanoparticle.

Effect of increasing concentration of nanoparticle on the emission spectra is shown in figure 5. Adding of nanoparticle to MMPI resulted quenching of its emission [Zhou, *et al., (2002)*]. The apparent association constants (K_{app}) have been obtained from the fluorescence quenching using the equation, $1/(F_0 - F) = 1/(F_0 - F) + 1/ K_{app} (F_0 - F)$ [nanoparticles], where K_{app} is the apparent association constant, F_0 is the initial fluorescence intensity of the MMPI, F is the maximum fluorescence intensity of the MMPI adsorbed on nanoparticle. A good linear relationship between $1/(F_0 - F)$and the reciprocal concentration of nanoparticle is seen (Figure 6). From the slope, the apparent association constants (K_{app}) have been assessed to binding of MMPI –nanoparticle.

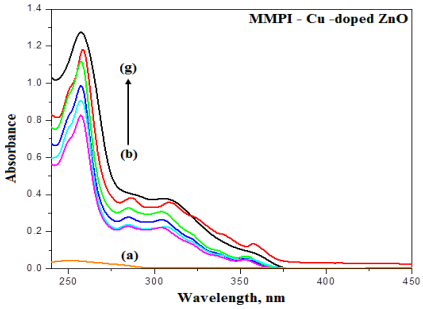

Absorption spectra of MMPI in presence and absence of different concentration of (a) Bare, (b)–(g) MPMPI and Cu –doped ZnO $1x10^{-5}M$ to $4.5x10^{-5}M$

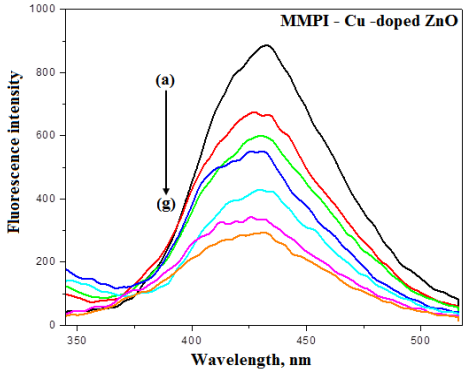

Fluorescence spectra of MMPI in presence and absence of different concentration of (a) Bare, (b)–(g) MPMPI and Cu –doped ZnO $1x10^{-5}M$ to $4.5x10^{-5}M$

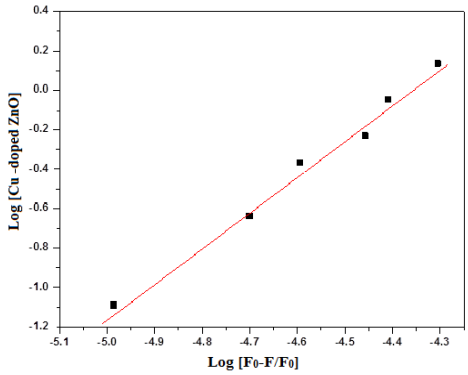

Stern-Volmer plot of log [F_0-F/F_0] versus [nanoparticle]

HOMO and LUMO energy levels of MMPI and Cu -doped ZnO

From the onset oxidation potential (E_{ox}) and the onset reduction potential (E_{red}) of the derivative, HOMO and LUMO energy level have been calculated using the equations [He, *et al., (2005)*], HOMO = $-e(E_{ox} + 4.71)$ (eV); LUMO = $-e(E_{red} + 4.71)$ (eV). On the basis of the relative HOMO and LUMO energy level of an isolated MMPI molecule along with the conduction band and valence band edges of Cu –doped ZnO nanoparticle as shown in Figure 7, the electron injection would be thermodynamically allowed from the excited singlet of the MMPI derivative to the conduction band of Cu –doped ZnO.The binding strength of MMPI through its nitrogen atom with Cu -doped ZnO is shown in figure (Figure 8). The fluorescence quenching process is confirmed to binding of MMPI with Cu -doped ZnO.

The thermodynamic feasibility of excited state electron transfer reaction has been confirmed by free energy change calculated by Rehm-Weller expression [Rehm, *et al., (1970)*], $\Delta G_{et} = E^{1/2}{}_{(ox)} - E^{1/2}{}_{(red)} - E_s + C$, where $E^{1/2}{}_{(ox)}$ is the oxidation potential of MMPI, $E^{1/2}{}_{(red)}$ is the reduction potential of Cu –doped ZnO nanoparticle, i.e., the conduction band potential of nanoparticle, E_s is the excited state energy of MMPI and Cis the coulombic term. Since the MMPI is neutral and the solvent used is polar in nature, the coulombic term in the above expression can be neglected [Parret, *et al., (1994)*]. The value of ΔG_{et} is calculated as −1.23 eV. The negative value indicates the thermodynamic feasibility of the electron transfer process.

Quenching arises between fluorophore and nanoparticles and the binding constants (*K*) have been calculated by using the equation, $\log [(F_0 - F)/F] = \log K + n$

log [nanoparticles], where K is the binding constant of nanoparticles with MMPI, which can be determined from the cut off log [(F_0– F)/F] versus log [nanoparticles] and the calculated value of binding constant K and number of binding sites (n) are given in Table 1. Binding of the MMPI to the nanoparticles surface is confirmed from the n value as one. Quenching process may also be due to the binding of MMPI with nanoparticle.

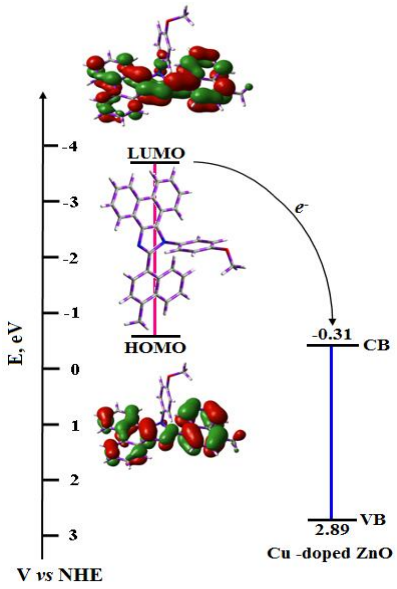

HOMO and LUMO energy levels of MMPI along with the CB and VB edge of Cu- doped ZnOnanoparticle

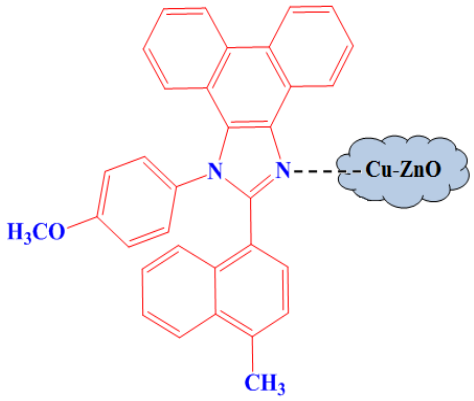

Schematic diagram describing the photoelectron transfer from MMPI to nanoparticle

Table 1.Parameters obtained by the interaction of MMPI with Cu-dopedZnO nanoparticle

Parameters	Cu-ZnO
K M^{-1}	6.39 x 10^7
n	1.67
ΔG_{et}	-1.23
J ($Cm^{-3}mol^{-1}$)	1.80x10^{-8}
R_0 (x 10^8m)	2.89
r_0 (nm)	27.8
E	0.61
k_{et}(x 10^8 s^{-1})	0.25

Molecular docking studies

To understand the binding interaction between biological macromolecule with 1-(4-methoxyphenyl)-2-(4-methylnaphthalen-1-yl)-1H-phenanthro[9,10-d]imidazole for the rational drug design and drug discovery molecular docking study has been carried out. By placing 1-(4-methoxyphenyl)-2-(4-methylnaphthalen-1-yl)-1H-phenanthro[9,10-d]imidazoleinto the binding site of the target specific region of the DNA mainly in a non-covalent fashion and to predict the correct binding mode and binding affinities [Haq, *et al.*, (2000)]. The more negative the binding energy the stronger is the interaction between 1-(4-methoxyphenyl)-2-(4-methylnaphthalen-1-yl)-1H-phenanthro[9,10-d]imidazole and DNA, the most stable the complex formed between 1-(4-methoxyphenyl)-2-(4-methylnaphthalen-1-yl)-1H-phenanthro[9,10-d] imidazole and DNA.

1-(4-methoxyphenyl)-2-(4-methylnaphthalen-1-yl)-1H-phenanthro[9,10-d] imidazole were successively docked with DNA duplex of sequence d(CGCGAATT CGCG)2 dodecamer (PDB ID: 1BNA) in order to expect the selected binding site along with favored orientation of the drug inside the DNA groove. The energetically favorable conformation of the docked pose exposed that 1-(4-methoxyphenyl)-2-(4-methylnaphthalen-1-yl)-1H-phenanthro[9,10-d] imidazole binds to groove of DNA (Figure 9). From the results (Table 2), it can be found that the binding free energy (DG) is apparently lower when there are adenine (A) and thymine (T) base pairs in the DNA sequences, indicating that the preferential binding site of 1-(4-methoxyphenyl)-2-(4-methylnaphthalen-1-yl)-1H-phenanthro[9,10-d] imidazole on the A-T rich sequence of DNA. However, 1-(4-methoxyphenyl)-2-(4-methylnaphthalen-1-yl)-1H-phenanthro[9,10-d] imidazole prefers to bind on the minor groove of A-T rich region of DNA molecule, which is reliable with above experimental results, and the considerable change of conformation of1-(4-methoxyphenyl)-2-(4-methylnaphthalen-1-yl)-1H-phenanthro[9,10-d]imidazole occurs in the binding process with DNA to orient easily along the minor groove.

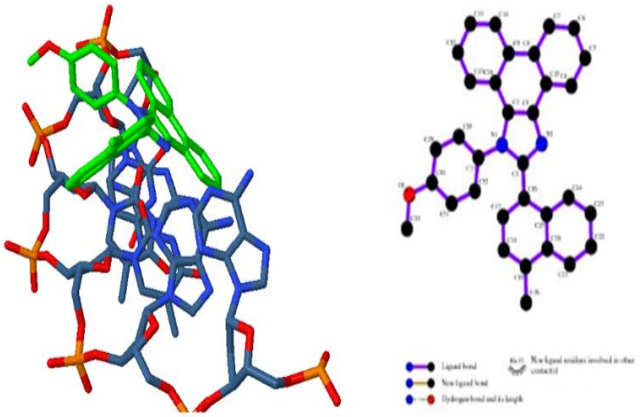

Molecular docking studies of 1-(4-methoxyphenyl)-2-(4-methylnaphthalen-1-yl)-1H-phenanthro[9,10-d]imidazole with DNA.

Table 2. Binding interaction energies of 1-(4-methoxyphenyl)-2-(4-methylnaphthalen-1-yl)-1H-phenanthro[9,10-d]imidazole with DNA

Conformation	BindingAffinity(Kcal/mol)
1	-6.11
2	-5.86
3	-5.64
4	-5.44
5	-5.16

Conclusions

Cu -doped ZnO nanoparticle prepared by sol-gel method and characterised by XRD, SEM, EDS, UV–visible spectroscopy and fluorescence spectra. The quenching process of MMPI is adsorbed on the surface of nanoparticle. Docking analysis shows that 1-(4-methoxyphenyl)-2-(4-methylnaphthalen-1-yl)-1H-phenanthro[9,10-d] imidazole prefer to bind on the minor groove of A-T rich region of DNA molecule.

Acknowledgments

Instrumentation facility will be provided by Department of Chemistry, Annamalai University, Annamalai nagar, is gratefully acknowledged. Dr. P. Ramanathan likes to thank the management of Thanthai Hans Roever College, Perambalur for the infrastructure and moral support.

References

Baker,S.N., Baker,A.G.,(2010),Luminescent Carbon Nanodots: Emergent Nanolights, *Angew. Chem., Int. Ed.49*, 6726–6744; Jaiswal,A.,Ghosh,S.S.,Chattopadhyay,A. (2012), One step synthesis of C-dots by microwave mediated caramelization of poly(ethylene glycol), *Chem. Commun.48*, 407–409.

Reineke,S., Lindner,F., Schwartz,G., Seidler,N.,Walzer,K.,Luessem,B.,Leo,K.,(2009), White organic light-emitting diodes with fluorescent tube efficiency, *Nature.459*, 234–238.

Vanithakumari,S.C., Nanda,K.K.,(2009),A One-Step

Method for the Growth of Ga_2O_3-Nanorod-Based White-Light-Emitting Phosphors, *Adv. Mater.21*, 3581–3584.

Wang,F., Chen,Y.H., Liu,C.Y.,Ma,D.G. (2011), White light-emitting devices based on carbon dots' electroluminescence, *Chem. Commun.47*, 3502–3504.

Sanju,K.S., Neelakandan,P.P.,Ramaiah,D.,(2011),DNA-assisted white light emission through FRET, *Chem. Commun.47*, 1288–1290.

Vohra,V.,Calzaferri,G.,Destri,S.,Pasini,M.,Porzio,W.,Botta, C. (2010),Toward white light emission through efficient two-step energy transfer in hybrid nanofibers, *ACS Nano.4*, 1409–1416.

Wang,X., Li,W.,Sun,K. (2011),Stable efficient CdSe/CdS/ZnS core/multi-shell nanophosphors fabricated through a phosphine-free route for white light-emitting-diodes with high color rendering properties, *J. Mater. Chem.21*, 8558–8565.

Vanheusden,K., Seager,C.H., Warren,W.L,.Tallant,D. RVoigt,, J.A. Correlation between photoluminescence and oxygen vacancies in ZnO phosphors, *Appl. Phys. Lett.68*, 403–405.

Van Dijken,A.,Meulenkamp, E.A.,Vanmaekelbergh,D. (2000),A. Meijerink, Influence of adsorbed oxygen on the emission properties of nanocrystalline ZnO particles, *J. Phys. Chem. B.104*, 4355–4360.

Johnston,H.J., Hutchison,G.R., Christensen,F.M., Peters,S.,Ankin,S., Stone,V. (2009),*Part. Fibre Toxicol.*6.

Sakohapa,S.,Tickazen,L.D., Anderson,M.A. (1992),Luminescence properties of thin zinc oxide membranes prepared by the sol-gel technique: change in visible luminescence during firing, *J. Phys. Chem.96*, 11086.

Harada,K.,Asakura,K., Ueki,Y.,Toshina,N. (1992),Structure of polymer-protected palladium-platinum bimetallic clusters at the oxidized state: extended x-ray absorption fine structure analysis, *J. Phys. Chem.96*, 9730.

Lee,J., Hwang,J.H.,Mashek,T.T., Mason,T.O. , Miller,A.E., Siegel,R.W. (1995),Impedance spectroscopy of grain boundaries in nanophase ZnO, *J. Mater. Res.10*, 2295.

K.,Horiguchi,T., Kinoshita,T.,Sayama,K. Sugihara,H. , Arakawa,H. (2000),Highly efficient photon-to-electron conversion with mercurochrome-sensitized nanoporous oxide semiconductor solar cells, *Solar Energy Mater. Solar Cells.64*, 115.

Cao, Jy. Xu,H. , Zhang,D.Z. (2000),Spatial Confinement of Laser Light in Active Random Media, *Phys. Rev. Lett.84*, 5584.

Bagnall,D.M., Chen,Y.F., Shen,M.Y.,. Zhu, Z.,Goto,T., Yao,T.J. (1998),*Cryst. Growth.605*, 184–185.

Xiong,H.M., Wang,Z.D.,Xia,Y.Y. (2006),Polymerization Initiated by Inherent Free Radicals on Nanoparticle Surfaces: A Simple Method of Obtaining Ultrastable (ZnO)Polymer Core–Shell Nanoparticles with Strong Blue Fluorescence, *Adv. Mater.18*, 748–751.

Xiong,H.M., Xu,Y., Ren,Q.G., and Xia,Y.Y. (2008),Stable aqueous ZnO@polymer core-shell nanoparticles with tunable photoluminescence and their application in cell Imaging, *J. Am. Chem. Soc.130*, 7522–7523.

Subramanian, V., Wolf,E.E.,Kamat,P.V. (2003),Green Emission to Probe Photoinduced Charging Events in ZnO-Au Nanoparticles. Charge Distribution and Fermi-Level Equilibration, *J. Phys. Chem. B. 107*, 7479–7485.

Frisch,M. J., Trucks,G. W., Schlegel,H. B.,Scuseria,G. E., Robb,M. A.,. Cheeseman, J. R ., Montgomery,J. A.,Vreven,T.,Kudin,K. N.,Burant,J. C.,Millam,J. M.,Iyengar,S. S.,Tomasi,J., Barone,V., Mennucci,B.,Cossi,M.,Scalmani,G.,Rega,N.,Petersson, G. A.,Nakatsuji,H.,Hada,M.,Ehara,M., Toyota,K., Fukuda,R. , Hasegawa, J. , Ishida,M. , Nakajima,T. , Honda,Y., Kitao,O.,Nakai,H.,Klene,M., Li,X., Knox, J. E., Hratchian,H. P., Cross,J. B., Bakken,V., Adamo,C., Jaramillo,J. , Gomperts, R.,. Stratmann,R. E,Yazyev, O. , Austin,A. J.,Cammi, R.,Pomelli,C. ,

Ochterski, J. W. , Ayala,P. Y.,Morokuma,K.,Voth,G. A., Salvador, P., Dannenberg,,J. J., Zakrzewski,V. G. ,Dapprich,S., Daniels,A. D. , Strain,M. C., Farkas,O.,Malick,D. K. , Rabuck,A. D.,Raghavachari,K., Foresman,J. B. , Ortiz,J. V., Cui,Q.,Baboul, A. G. , Clifford,S. ,Cioslowski,J.,Stefanov,B. B. , Liu,G. ,Liashenko,A. ,Piskorz,P. ,Komaromi,I. , Martin,R. L. , Fox,D. J. , Keith,T. , Al-Laham,M. A. , Peng,C. Y. ,Nanayakkara,A. ,Challacombe,M. , Gill,P. M. W. , Johnson,B. ,Chen, W. , Wong,M. W. , Gonzalez,C. , Pople, J. A. (2004),Gaussian 03 (Revision E.01), Gaussian, Inc., Wallingford, CT.

Ojha,P.K., Roy, K. (2010), Chemometric modeling, docking and in silico design of triazolopyrimidine-based dihydroorotate dehydrogenase inhibitors as antimalarials, *Eur. J. Med. Chem. 45*, 4645-4656.

Morris,G.M. ,Goodsell,D.S. , Halliday, R.S. , Huey,R. , Hart,W.E. ,Belew,R.K. , Olson,A.J. (1998), Automated docking using a Lamarckian genetic algorithm and an empirical binding free energy function, *J. Comput. Chem.19*, 1639-1662.

Morris,G.M. , Huey,R. , Lindstrom, W.,Sanner,M.F. ,Belew,R.K. ,Goodsell,D.S. , Olson,A.J. (2009), AutoDock4 and AutoDockTools4: Automated docking with selective receptor flexibility, *J. Comput. Chem.30*, 2785-2791.

Huey, R. Morris,G.M, A.J. Olson, D.S. Goodsell, (2007), A semiempirical free energy force field with charge-based desolvation, *J. Comput. Chem.*28, 1145-1152.

De Lano,W.L. (2004), The PyMOL Molecular Graphics System, *De Lano Scientific. San Carlos,CA.*

(a)Zhou,Z., Qian,S., Yao,S.,Zhang,Z. (2002),Electron transfer in colloidal TiO_2 semiconductors sensitized by hypocrellin A, *Radiat. Phys. Chem.65*, 241–248; (b)Huber,C.,Fähnrich,K., Krause,C.,Werner,T. (1999),Synthesis and characterization of new chloride-sensitive indicator dyes based on dynamic fluorescence quenching, *J. Photochem. Photobiol. A: Chem.128*, 111-120.

He,W.Y., Li,Y.,Xue ,C., Hu,Z.D., Chen,X.G., Sheng,F.L. (2005),Effect of Chinese medicine alpinetin on the structure of human serum albumin, *Bioorg. Med. Chem.13*,1837-1845.

Rehm,D., Weller,A. (1970),Kinetics of Fluorescence Quenching by Electron and H-Atom Transfer, *Isr. J. Chem.8*, 259-271.

Parret,S.,Savary,F.M.,Fouassier,J.P., Ramamurthy,P. (1994),MND In-orbit-coupling-induced triplet formation of triphenylpyrylium ion: a flash photolysis study, *J. Photochem. Photobiol. A. 83*, 205–209.

Haq,I.,Ladbury,J. (2000), Drug–DNA recognition: energetics and implications for design, *J. Mol. Recogn.13*, 188-197.